Journal of Applied Mechanics Vol. 4, pp. 295-306 (August 2001) JSCE

Nonlinear analysis for stress-strain-strength of clays using return-mapping algorithms

Thirapong PIPATPONGSA*, Atsushi IIZUKA **, Ichizo KOBAYASHI***, Hideki OHTA**** and Yukihito SUZUKI*****

*Dept. of International Development Eng., Tokyo Institute of Technology, O-okayama, Meguro-ku, Tokyo 152-8550
** Dr. of Eng., Assoc. Prof., Dept. of Civil Eng., Kobe University, Rokkodai-cho, Nada-ku, Kobe 657-8501
*** Dr. of Eng., Research Associate, Dept. of Civil Eng., Tokyo Institute of Technology, O-okayama, Meguro-ku, Tokyo 152-8550
**** Dr. of Eng., Prof., Dept. of International Development Eng., ditto
***** Senior Researcher, Center for Computational Science and Engineering,
Fuji Research Institute Corporation, Kandanishiki-chou, Chiyoda-ku, Tokyo, 101-8443

The infinitesimal deformation analysis of the rate-independent Sekiguchi-Ohta model is formulated to include a class of two-invariant stored energy function considering initial state of stress. Elastic shear modulus is assumed to depend on pre-consolidation pressure and increase exponentially with strain-hardening parameter after yielding by taking damage effect on energy conservation into account. The principle of maximum plastic dissipation is connected to the associated flow rule while hardening/softening law is described by the hardening potential function defined to suit the model. The implicit integrative scheme is return mapping algorithm based on the Closest Point Projection method. The nonlinear analyses for stress-strain-strength under UU and CU tests were carried out to test the performance. It was found that the method is proven to robust, stable and accurate even in very large strain increments.

Key Words: closest point projection method, return-mapping algorithm, numerical integration, elasto-plasticity

1. Introduction

In the realm of nonlinear analysis for cohesive soils, the model proposed by Sekiguchi and Ohta[1] (1977) is one of the most widely used soil constitutive models based on Critical State theory. The model characterizes nonlinear stress-strain behavior including softening/hardening and dilatancy responses, principal stress reorientation, initial-stress-induced anisotropy and time dependency. The performance of the model has been proved to be consistent with many field responses in predicting soil behaviors (Ohta and Iizuka[2], 1992). The integration of constitutive equation over a discrete sequence of time step is commonly practiced by incremental solution that is classified into explicit and implicit categories. The first method simplifies the integration to the summation of sub-increments while the latter one applies the iterative scheme using Newton-Raphson method formulated in complex expressions. It has been shown that the procedure used for explicitly integrating the constitutive equations is inferior to that of implicit integration on solution stability and accuracy[3]. Moreover, in nonlinear problem, the size of increments substantially affect the quality of analysis, that is, a large step size will cause inaccuracy while a finer one will become a drawback in computation speed. According to several literatures[4-5], the effective method suggested to handle the problems is to apply the implicit integration method using return-mapping algorithm, the algorithm that usually starts in the first iteration with a purely elastic increment.

Much of foundation for the return-mapping methods for nonlinear isotropic and kinematic hardening/softening plasticity have been contributed over the passed two decade (Simo et al[6-9], 1985, 1988, 1992, 1993) in which Closest Point Projection (CPP) and Cutting-Plane (CP) methods have been developed.

Borja et al[10-13] (1990, 1991, 1998, 2001) have developed the implementation of return-mapping algorithms applicable to the modified Cam-Clay model with a remarkable solution accuracy and quadratic rate of convergence. However, the procedures concerned show a sign of incompatibility with the Sekiguchi-Ohta model because both models have lost much in

common since the advent of modified version. In addition, a number of recent studies have been proposed for the modified Cam-clay with prominent performance.

Recently, Pipatpongsa and Ohta[14] (2000) developed the return-mapping algorithm applicable to an invisid form of the Sekiguchi-Ohta model as its first kind of implementation, which is fallen within the class of convex CP method coupled nonlinear hypoelastic response on two invariants stress space. The iterative return path generated by the algorithm is optimized at quadratic rate with high accuracy.

The purpose of this paper is to extend the previous work by developing an efficient CPP method applicable to the Sekiguchi-Ohta plasticity model, formulated to include a class of two-invariant stored energy function considering initial stress and damage process. The nonlinear elasticity is adopted by taking shear modulus G varied with pre-consolidation pressure while bulk modulus K is varied with mean stress. As a consequence, a conservation of energy is satisfied and path independent feature can be guaranteed in an elastic predictor step, which is rigorously required by return mapping algorithms.

An outline of the paper is as follows. In section 2, the mathematical framework is set for the algorithmic residuals and constraints. The constitutive equations and empirical hardening law are reviewed in section 3. Section 4 deals with a class of stored energy function considering initial stress. In section 5, hardening potential function appropriate with the model is defined. A procedure for damage process is accounted for changing a value of G in corresponding to a hardening parameter. A set of equations regulating the elastic constitutive law is arranged in section 6. In section 7, the implicit integrative scheme under CPP method is derived. In section 8, the nonlinear analysis for stress-strain-strength under CU and UU tests in two-invariant stress space problem were carried out to test the performance of the algorithm by comparing with sub-stepping technique and closed-form solutions. The conclusion is marked in section 9.

It is noted that in this study, attention is confined to infinitesimal deformation and rate-independent plasticity. It is out of scope in this paper to consider the existence of corner on yield surface however basic theories[7] and ongoing researches are available[15-18]. The unusual procedures can be neglected if the interested stress points lie outside and far from the corner. The further research subjected to soil/water coupling FEM for three-dimensional state of stress is being developed.

2. Plastic dissipation

This section illustrates the important role of the principle of maximum plastic dissipation[19] (Hill, 1950), its connection to the associated flow rule[20] (Drucker's stability or normality postulate, 1950) and basic regularization in the infinitesimal elasto-plasticity. The mathematical framework advocated by Simo[8] (1992) is rephrased but a modification is made for plastic variables in a sense to suit the hardening potential function defined in the section 5. Within a convex elastic domain of stress space defined by

$$\mathbb{E} \equiv \left\{ (\boldsymbol{\sigma}, h) \in \mathbb{S} \times R^{+} \,\middle|\, f(\boldsymbol{\sigma}, h) \le 0 \right\} \tag{2.1}$$

where $\mathbb{S}$ is a vector space of symmetric second-order tensors, R^{+} is a real range of positive number and h is a stress-like hardening parameter of material. Based on the 2nd Law of Thermodynamics, partially a universal law of decay, the dissipation function is defined by the difference between the stress power and the rate of change of the internal energy. The symbol ':' signifies the contraction of a tensor by 2 orders.

$$\mathscr{D} = \boldsymbol{\sigma} : \dot{\boldsymbol{\varepsilon}} - \dot{\Psi}(\boldsymbol{\varepsilon}^{e}, \alpha) \ge 0 \tag{2.2}$$

The internal energy is composed of elastic and hardening plastic components expressed by the stored energy function and hardening potential; i.e.,

$$\nabla_{\boldsymbol{\varepsilon}^{e}} \Psi = \psi(\boldsymbol{\varepsilon}^{e}, \alpha), \qquad \nabla_{\alpha} \Psi = \mathscr{H}(\alpha) \tag{2.3a, b}$$

The stored energy function and hardening potential function are subjected to define in section 4 and 5. The stress responses can be obtained by hyperelastic relationship. Herein, α denotes a strain-like variable conjugating to a material memory variable h.

$$\boldsymbol{\sigma} = \frac{\partial \psi(\boldsymbol{\varepsilon}^{e}, \alpha)}{\partial \boldsymbol{\varepsilon}^{e}}, \qquad h = \frac{\partial \mathscr{H}(\alpha)}{\partial \alpha} \tag{2.4a, b}$$

Using Eq.(2.3a, b) and chain rule to Eq.(2.2) yields,

$$\mathscr{D} = [\boldsymbol{\sigma} - \nabla_{\boldsymbol{\varepsilon}^{e}} \psi] : \dot{\boldsymbol{\varepsilon}} + \nabla_{\boldsymbol{\varepsilon}^{e}} \psi : \left[\dot{\boldsymbol{\varepsilon}} - \dot{\boldsymbol{\varepsilon}}^{e} \right] - \partial_{\alpha} \mathscr{H}(\alpha) \dot{\alpha} \ge 0 \tag{2.5}$$

Eq. (2.4a-b, 2.5) imply (2.6) to hold for all admissible stress state and hence the optimum stress state for a given strain rate can be obtained by maximizing,

$$\text{Objective function: } \mathscr{D} = \boldsymbol{\sigma} : \left[\dot{\boldsymbol{\varepsilon}} - \dot{\boldsymbol{\varepsilon}}^{e} \right] - h\dot{\alpha} \ge 0 \tag{2.6}$$

Optimized variable: $(\boldsymbol{\sigma}, h) \in \dot{\mathbb{E}}$

Subject to constraint: $f(\boldsymbol{\sigma}, h) \le 0$

The corresponding Lagrangian function

$$L = -\mathscr{D} + \gamma . f(\boldsymbol{\sigma}, h) \tag{2.7}$$

By Kuhn-Tucker condition for extrema, define the residuals

$$\nabla L = \begin{Bmatrix} \nabla_{\boldsymbol{\sigma}} L \\ \nabla_{h} L \end{Bmatrix} = \begin{Bmatrix} -\left[\dot{\boldsymbol{\varepsilon}} - \dot{\boldsymbol{\varepsilon}}^{e} \right] + \gamma \dfrac{\partial f}{\partial \boldsymbol{\sigma}} \\ \dot{\alpha} + \gamma \dfrac{\partial f}{\partial h} \end{Bmatrix} = \begin{Bmatrix} \mathbf{0} \\ 0 \end{Bmatrix} \tag{2.8a, b}$$

$$\gamma \ge 0 \; ; f(\boldsymbol{\sigma}, h) \le 0 \; ; \gamma . f(\boldsymbol{\sigma}, h) = 0 \tag{2.9a, b, c}$$

Eq.(2.8a, b) are read as associative flow rule and associative hardening/softening law to the maximum dissipation energy principle. It is noted that Eq.(2.9a-c) can judge

loading/unloading condition but can not judge for a state of hardening/softening.

$$\dot{\boldsymbol{\varepsilon}}^{p} = \dot{\boldsymbol{\varepsilon}} - \dot{\boldsymbol{\varepsilon}}^{e} = \gamma \frac{\partial f}{\partial \boldsymbol{\sigma}}, \qquad \dot{\alpha} = -\gamma \frac{\partial f}{\partial h} \qquad (2.10a, b)$$

Eq. (2.10a) is corresponding to the postulate of associated flow rule by taking a Lagrangian multiplier γ as proportionality constant. In Critical state models, a hardening plastic variable h is chosen to p'_c and its conjugate α is referred to ε^{p}_{v} in particular. Therefore, an empirical hardening law denoted in Eq.(2.11) is commonly employed instead. Comparison of Eq.(2.10b) to Eq. (2.11) implies the adopted hardening/softening law in Critical state models is non-associative sense[9),13)], that is, Lagrangian function in Eq.(2.7) is not maximized because α is empirically associated to volumetric plastic strain, not theoretically associated to p'_c.

$$\dot{\alpha} = \dot{\varepsilon}^{p}_{v} = \dot{\boldsymbol{\varepsilon}}^{p} : \mathbf{1} = \gamma \frac{\partial f}{\partial p'} \neq -\gamma \frac{\partial f}{\partial h} \qquad (2.11)$$

Eq.(2.10a) is found to contain (2.11), therefore, hardening parameter updating procedure can be set aside from iteration as formulated in section 7.

3. Constitutive laws

Sekiguchi and Ohta (1977) proposed constitutive equations for stress-induced anisotropy in clays. The inviscid form of yield function is expressed by

$$\mathrm{f}(\boldsymbol{\sigma}, p'_c) \equiv f(p', \eta^{*}, p'_c) = MD \ln\left(\frac{p'}{p'_c}\right) + D\eta^{*} = 0 \quad (3.1)$$

p'_c indicates an isotropic hardening stress of the subsequent yield surface which is determined by an empirical relationship based on *e-ln(p')* curves of consolidation test (Eq. 3.2- 3.3).

$$\varepsilon^{p}_{v} - \varepsilon^{p}_{vo} = \frac{\lambda - \kappa}{1 + e_o} \ln\left(\frac{p'_c}{p'_o}\right) \qquad (3.2)$$

$$\varepsilon^{e}_{vc} - \varepsilon^{e}_{vco} = \frac{\kappa}{1 + e_o} \ln\left(\frac{p'_c}{p'_o}\right) \qquad (3.3)$$

The pre-consolidation pressure p'_o marks the isotropic pressure after the completion of K_o-consolidation. According to an infinitesimal void ratio-volumetric strain relationship denoted in Eq.(3.4a), the plastic and elastic volumetric strain at p'_o equal to zero, Eq.(3.4b-c).

$$\dot{\varepsilon}_{v} = \frac{-\dot{e}}{1 + e_o}, \quad \varepsilon^{p}_{vo} = 0, \quad \varepsilon^{e}_{vco} = 0 \qquad (3.4a, b, c)$$

Select the candidates of hardening variables in particular

$$h = p'_c, \quad \alpha = \varepsilon^{p}_{v} \qquad (3.5a, b)$$

where recompressibility and compressibility indices are

$$\bar{\kappa} = \frac{\kappa}{1 + e_o}, \qquad \bar{\lambda} = \frac{\lambda}{1 + e_o} \qquad (3.6a, b)$$

A summary of constitutive laws is noted in Box 1.

Box 1: Constitutive equations

Yield function proposed by Sekiguchi and Ohta (1977)

$$\mathrm{f}(\boldsymbol{\sigma}, p'_c) \equiv f(p', \eta^{*}, p'_c) = MD \ln\left(\frac{p'}{p'_c}\right) + D\eta^{*} = 0$$

where $p' = \frac{1}{3} tr(\boldsymbol{\sigma})$; $p'_o = \frac{1}{3} tr(\boldsymbol{\sigma}_o)$; $\mathbf{s} = \boldsymbol{\sigma} - p'\mathbf{1}$

$$\mathbf{s}_o = \boldsymbol{\sigma}_o - p'_o \mathbf{1} ; \boldsymbol{\eta} = \frac{\mathbf{s}}{p'} ; \boldsymbol{\eta}_o = \frac{\mathbf{s}_o}{p'_o} ; \eta^{*} = \sqrt{\frac{3}{2}} \|\boldsymbol{\eta} - \boldsymbol{\eta}_o\|$$

$$q = \sqrt{\frac{3}{2}} \|\mathbf{s}\| ; \eta_o = \frac{3(1 - K_o)}{1 + 2K_o} ; D = \frac{\lambda - \kappa}{M(1 + e_o)}$$

In generalized convex format

$$\mathrm{f}(\boldsymbol{\sigma}, p'_c) \equiv f(I_1, \bar{J}_2, I_c) = MD \ln\left(\frac{I_1}{I_c}\right) + D\frac{\sqrt{27\bar{J}_2}}{I_1} = 0$$

where $\bar{\mathbf{s}} = \mathbf{s} - p'\boldsymbol{\eta}_o$; $I_1 = \mathbf{1} : \boldsymbol{\sigma}$; $\bar{J}_2 = \frac{1}{2} tr(\bar{\mathbf{s}}^2)$; $I_c = 3p'_c$

$$\mathbf{I} \equiv \frac{1}{2}\left[\delta_{ik}\delta_{jl} + \delta_{il}\delta_{jk}\right] \mathbf{e}_i \otimes \mathbf{e}_j \otimes \mathbf{e}_k \otimes \mathbf{e}_l$$

$$\mathbf{A} \equiv \mathbf{I} - \frac{1}{3}(\mathbf{1} \otimes \mathbf{1}) ; \ \mathbf{1} \equiv \delta_{ij} \mathbf{e}_i \otimes \mathbf{e}_j$$

$$\bar{\mathbf{A}} \equiv \mathbf{A} - \frac{1}{3}\mathbf{1} \otimes \boldsymbol{\eta}_o - \frac{1}{3}\boldsymbol{\eta}_o \otimes \mathbf{1} + \frac{1}{9}\boldsymbol{\eta}_o : \boldsymbol{\eta}_o (\mathbf{1} \otimes \mathbf{1})$$

First derivative of yield function

$$\frac{\partial f}{\partial \boldsymbol{\sigma}} = \frac{\partial f}{\partial I_1}\frac{\partial I_1}{\partial \boldsymbol{\sigma}} + \frac{\partial f}{\partial \bar{J}_2}\frac{\partial \bar{J}_2}{\partial \boldsymbol{\sigma}}$$

where $\frac{\partial I_1}{\partial \boldsymbol{\sigma}} = \mathbf{1}$; $\frac{\partial \bar{J}_2}{\partial \boldsymbol{\sigma}} = \left(\mathbf{A} - \frac{1}{3}\mathbf{1} \otimes \boldsymbol{\eta}_o\right) : \bar{\mathbf{s}} = \bar{\mathbf{A}} : \boldsymbol{\sigma}$

$$\frac{\partial f}{\partial I_1} = \frac{D}{I_1}\left(M - 3\frac{\sqrt{3\bar{J}_2}}{I_1}\right) ; \frac{\partial f}{\partial \bar{J}_2} = \frac{9D}{2I_1\sqrt{3\bar{J}_2}}$$

Second derivative of yield function

$$\frac{\partial^2 f}{\partial \boldsymbol{\sigma}\partial \boldsymbol{\sigma}} = \frac{\partial^2 f}{\partial \boldsymbol{\sigma}\partial I_1} \otimes \frac{\partial I_1}{\partial \boldsymbol{\sigma}} + \frac{\partial^2 f}{\partial \boldsymbol{\sigma}\partial \bar{J}_2} \otimes \frac{\partial \bar{J}_2}{\partial \boldsymbol{\sigma}} + \frac{\partial f}{\partial I_1}\frac{\partial^2 I_1}{\partial \boldsymbol{\sigma}\partial \boldsymbol{\sigma}} + \frac{\partial f}{\partial \bar{J}_2}\frac{\partial^2 \bar{J}_2}{\partial \boldsymbol{\sigma}\partial \boldsymbol{\sigma}}$$

where $\frac{\partial^2 I_1}{\partial \boldsymbol{\sigma}\partial \boldsymbol{\sigma}} = \mathbf{0}$; $\frac{\partial^2 \bar{J}_2}{\partial \boldsymbol{\sigma}\partial \boldsymbol{\sigma}} = \bar{\mathbf{A}}$

$$\frac{\partial^2 f}{\partial \boldsymbol{\sigma}\partial I_1} = \frac{\partial^2 f}{\partial I_1 \partial I_1}\frac{\partial I_1}{\partial \boldsymbol{\sigma}} + \frac{\partial^2 f}{\partial \bar{J}_2 \partial I_1}\frac{\partial \bar{J}_2}{\partial \boldsymbol{\sigma}}$$

$$\frac{\partial^2 f}{\partial \boldsymbol{\sigma}\partial \bar{J}_2} = \frac{\partial^2 f}{\partial I_1 \partial \bar{J}_2}\frac{\partial I_1}{\partial \boldsymbol{\sigma}} + \frac{\partial^2 f}{\partial \bar{J}_2 \partial \bar{J}_2}\frac{\partial \bar{J}_2}{\partial \boldsymbol{\sigma}}$$

$$\frac{\partial^2 f}{\partial I_1 \partial I_1} = -\frac{MD}{I_1^{\,2}} + \frac{6D\sqrt{3\bar{J}_2}}{I_1^{\,3}} ; \frac{\partial^2 f}{\partial \bar{J}_2 \partial I_1} = -\frac{9D}{2I_1^{\,2}\sqrt{3\bar{J}_2}}$$

$$\frac{\partial^2 f}{\partial I_1 \partial \bar{J}_2} = -\frac{9D}{2I_1^{\,2}\sqrt{3\bar{J}_2}} ; \frac{\partial^2 f}{\partial \bar{J}_2 \partial \bar{J}_2} = -\frac{9D}{4I_1\bar{J}_2\sqrt{3\bar{J}_2}}$$

4. Nonlinear elasticity

Mechanisms of strain are typically depicted by recoverable and irrecoverable parts caused by alternation in particle spacing, bending and reorientation of clay particles. Elastic stress-strain relation should cover time independent behavior, recoverable feature (monotonic & hysteretic) and small strain range. Classes of soil elasticity are among of linear, nonlinear, isotropic, anisotropic hypoelasticity and hyperelasticity. Hypoelasticity (Cauchy's elasticity) is fine for monotonic unloading/reloading but not guaranteed in energy conservation and path dependence. Hyperelasticity (Green's elasticity) is acceptable for all types of unloading/reloading, satisfying conservation of energy in any closed loop and path independence. In regardless of stiffness degradation by small strain, the typical elastic constitutive equation is related to volumetric and deviatoric stress-strain responses with stress variable stiffness as shown in Eq.(4.1).

$$\begin{Bmatrix} \dot{p}' \\ \dot{q} \end{Bmatrix} = \begin{bmatrix} K & J \\ J & 3G \end{bmatrix} \begin{Bmatrix} \dot{\varepsilon}_v^e \\ \dot{\varepsilon}_s^e \end{Bmatrix} \tag{4.1}$$

For materials that are elastic and isotropic, the coupled shear and volumetric effects are decoupled; i.e., J equals to zero[21]. Isotropic pressure-dependent bulk and shear moduli; i.e., *K=K(p'), G=G(p')* are often employed but such relation does not give an energy conservative model[22-23]. Thus, the viable nonlinear elastic moduli are restricted to a sort of *K=K(p')* and constant *G* [24]. Actually, an extensive study showed that G is both a function of p' and p'_c [25]. For an illustrative study, G is assumed to depend only on p'_c and governed by a stored energy function cast for a class of two-invariant isotropic nonlinear hyperelasticity accounted for damage effects. Energy conservation is guaranteed in the elastic domain but the material characteristics on the subsequent state boundary are path dependence and obeyed the elasto-plastic constitutive laws. The damage process is incorporated when elastic domain changes in shape due to hardening/softening process.

It is noted that a sort of *K=K(p')* and *G= G(p'c)* implies a variation of apparent Poisson's ratio which may become very low or negative value for a considerably low mean stress. Thus, there is a limitation of applying *G(p'c)* to a certain extent of OCR values. To solve this difficulty, a light of *K=K(p',q)* and *G=G(p')* has come into view in recent research[25-26], though, complex expressions of non-zero coupling modulus J and elastic dilatancy response during simple shear appear questionable.

By and large, soil is considered to hold initial stresses, thus, work done by initial stresses is included to the stored energy. The parameter of hardening p'_c is held constant in formulation.

4.1 Energy of distortion

Consider the energy as a product of deviatoric stress-strain,

$$\chi(\varepsilon_s^e, p'_c) \equiv \frac{1}{2}(\mathbf{s} - \mathbf{s}_i)^T \cdot \boldsymbol{\varepsilon}_d^e + \mathbf{s}_i^T \cdot \boldsymbol{\varepsilon}_d^e \tag{4.2}$$

where ε^e_d is the principal elastic strain deviator, s is the principal stress deviator. s_i is initial stress deviator, q_i stands for initial deviatoric stress and *G(p'c)* denotes the shear modulus. Eq.(4.2) can be reduced to,

$$\chi(\varepsilon_s^e, p'_c) = \frac{3}{2} G(p'_c) \varepsilon_s^{e\,2} + q_i \varepsilon_s^e \tag{4.3}$$

where $\varepsilon_s^e = \sqrt{\frac{2}{3}} \left\| \boldsymbol{\varepsilon}_d^e \right\|$, $\boldsymbol{\varepsilon}_d^e \equiv \boldsymbol{\varepsilon}^e - \varepsilon_v^e \cdot \mathbf{1}$, $q_i = \sqrt{\frac{3}{2}} \left\| \mathbf{s}_i \right\|$

Conjugate of χ by Legendre transformation

$$\bar{\chi}(q, p'_c) = \max_{\varepsilon_s} (q.\varepsilon_s^e - \chi(\varepsilon_s^e)) = \frac{1}{6} \frac{(q - q_i)^2}{G(p'_c)} \tag{4.4}$$

4.2 Energy of contraction

Based on *e-ln(p')* curve of consolidation test,

Void ratio-strain relation (elastic): $\dot{\varepsilon}_v^e = \frac{-\dot{e}}{1 + e_o}$ (4.5)

e_o is the reference state referred to void ratio at the completion of consolidation.

Elastic swelling curve: $\dot{e} = -\frac{\kappa}{p'} \dot{p}'$ (4.6)

Initial condition: $\varepsilon_v^e(p'_i) = \varepsilon_{vi}^e \equiv 0$ (4.7)

Substitute Eq.(4.6) into (4.5), integrate with initial condition

$$\varepsilon_v^e = \frac{\kappa}{1 + e_o} \ln\left(\frac{p'}{p'_i}\right) \tag{4.8}$$

Rewrite Eq.(4.8) to $p' = p'_i \exp\left(\frac{\varepsilon_v^e - \varepsilon_{vi}^e}{\bar{\kappa}}\right)$ (4.9)

Form potential strain energy by setting: $p' = \frac{\partial U}{\partial \varepsilon_v^e}$ (4.10)

Integrating Eq.(4.10) reveals the potential energy as follow,

$$U - U_i = \int_{\varepsilon_{vi}^e}^{\varepsilon_v^e} p' \, d\varepsilon_v^e = p'_i \, \bar{\kappa} \exp\left(\frac{\varepsilon_v^e - \varepsilon_{vi}^e}{\bar{\kappa}}\right) \tag{4.11}$$

Potential energy is energy of state. And the state chosen to correspond to zero potential energy is arbitrary. As a consequence, the constant terms in (4.11) is omitted,

$$U = p'_i \, \bar{\kappa} \exp\left(\frac{\varepsilon_v^e - \varepsilon_{vi}^e}{\bar{\kappa}}\right) \tag{4.12}$$

Find a conjugate of U by using Legendre transformation,

$$W = p' \bar{\kappa} \left[\ln\left(\frac{p'}{p'_i}\right) + \frac{\varepsilon_{vi}^e}{\bar{\kappa}} - 1 \right] \tag{4.13}$$

4.3 Stored energy function

Sum of Eq.(4.3) and (4.12) gives a stored energy function as

presented by Eq.(4.14) below

$$\psi(\varepsilon_v^e, \varepsilon_s^e, p'_c) = p'_i \bar{\kappa} \exp(\frac{\varepsilon_v^e - \varepsilon_{vi}^e}{\bar{\kappa}}) + \frac{3}{2} G(p'_c) \varepsilon_s^{e2} + q_i \varepsilon_s^e$$

Complementary stored energy function is also obtained,

$$\varpi(p', q, p'_c) = p' \bar{\kappa} \left[\ln(\frac{p'}{p'_i}) + \frac{\varepsilon_{vi}^e}{\bar{\kappa}} - 1 \right] + \frac{1}{6} \frac{(q - q_i)^2}{G(p'_c)} \quad (4.15)$$

Stress relation can be taken by gradient of stored energy

$$\begin{Bmatrix} p' \\ q \end{Bmatrix} = \nabla\psi = \begin{Bmatrix} \frac{\partial\psi}{\partial\varepsilon_v^e} \\ \frac{\partial\psi}{\partial\varepsilon_s^e} \end{Bmatrix} = \begin{Bmatrix} p'_i \exp(\frac{\varepsilon_v^e - \varepsilon_{vi}^e}{\bar{\kappa}}) \\ 3G(p'_c)\varepsilon_s^e + q_i \end{Bmatrix} \quad (4.16)$$

By the same fashion, strain relation is,

$$\begin{Bmatrix} \varepsilon_v^e \\ \varepsilon_s^e \end{Bmatrix} = \nabla\varpi = \begin{Bmatrix} \frac{\partial\varpi}{\partial p'} \\ \frac{\partial\varpi}{\partial q} \end{Bmatrix} = \begin{Bmatrix} \bar{\kappa} \ln(\frac{p'}{p'_i}) + \varepsilon_{vi}^e \\ \frac{1}{3} \frac{q - q_i}{G(p'_c)} \end{Bmatrix} \quad (4.17)$$

Stiffness matrix can be taken via stored energy function as

$$\mathbf{C} \equiv \nabla\nabla\psi = \begin{bmatrix} \frac{\partial^2\psi}{\partial p'^2} & \frac{\partial^2\psi}{\partial q \partial p'} \\ \frac{\partial^2\psi}{\partial p' \partial q} & \frac{\partial^2\psi}{\partial q^2} \end{bmatrix} \quad (4.18)$$

$$\text{Then} \quad \mathbf{C} = \begin{bmatrix} \frac{p'_i}{\bar{\kappa}} \exp(\frac{\varepsilon_v^e - \varepsilon_{vi}^e}{\bar{\kappa}}) & 0 \\ 0 & 3G(p'_c) \end{bmatrix} \quad (4.19)$$

By the same fashion, the compliance matrix is

$$\mathbf{E} = \mathbf{C}^{-1} = \nabla\nabla\varpi = \begin{bmatrix} \frac{\bar{\kappa}}{p'} & 0 \\ 0 & \frac{1}{3G(p'_c)} \end{bmatrix} \quad (4.20)$$

Compare Eq.(4.1) with (4.19) and (4.20), tangent bulk modulus is determined by,

$$K(\varepsilon_v^e) = \frac{p'_i}{\bar{\kappa}} \exp(\frac{\varepsilon_v^e - \varepsilon_{vi}^e}{\bar{\kappa}}) \quad \text{or} \quad K(p') = \frac{p'}{\bar{\kappa}} \quad (4.21)$$

Tangent shear modulus is set to be the function of constant Poisson's ratio ν' and bulk modulus at the state of consolidation,

$$G(p'_c) = \mu' K(p'_c) = \mu' \frac{p'_c}{\bar{\kappa}} \quad (4.22)$$

$$\text{where} \quad \mu' = \frac{3(1 - 2\nu')}{2(1 + \nu')} \quad (4.23)$$

In Eq.(4.24), the parameter p'_c can be calculated from a pre-consolidation pressure p'_o and volumetric plastic strain ε^p_v or volumetric elastic strain ε^e_{vc} in loading process or consolidation on *e-ln(p')* relation (see Eq.(3.2-3.4)). The rate form of p'_c will be discussed later. The change of p'_c causes a change in size of elastic domain and trigger damage process on stored energy.

$$p'_c = p'_o \exp(\frac{\varepsilon_v^p}{\bar{\lambda} - \bar{\kappa}}) = p'_o \exp(\frac{\varepsilon_{vc}^e}{\bar{\kappa}}) \quad (4.24)$$

It is concluded that, within state boundary condition, G is constant but increase exponentially with strain-hardening parameter after yielding by taking damage effect on energy conservation into account. Its explicit evaluation will be shown in the next section.

5. Hardening potential and Inelastic damage process

Irreversible part of isotropic normal compression represents the hardening development in soil particles. A hardening potential function is defined to keep in line with a stored energy of volumetric elastic strains Eq.(4.12). Under this combining process, an internal energy and derivative can be defined straightforward by,

$$\mathcal{H}(\alpha) = p'_o (\bar{\lambda} - \bar{\kappa}) \exp(\frac{\alpha}{\bar{\lambda} - \bar{\kappa}}) \quad (5.1)$$

$$\dot{\mathcal{H}}(\alpha) = \frac{\dot{\alpha}}{\bar{\lambda} - \bar{\kappa}} \mathcal{H}(\alpha) \quad (5.2)$$

Substituting Eq.(5.1) into Eq.(2.4b) yields a stress-hardening parameter corresponds to Eq.(3.5a).

$$h = p'_o \exp(\frac{\alpha}{\bar{\lambda} - \bar{\kappa}}) = p'_c \quad (5.3)$$

Nonlinear plastic modulus and rate form of p'_c are obtained by

$$H(p'_c) = \frac{p'_c}{\bar{\lambda} - \bar{\kappa}}, \quad \dot{p}'_c = H(p'_c)\dot{\alpha} \quad (5.4a, b)$$

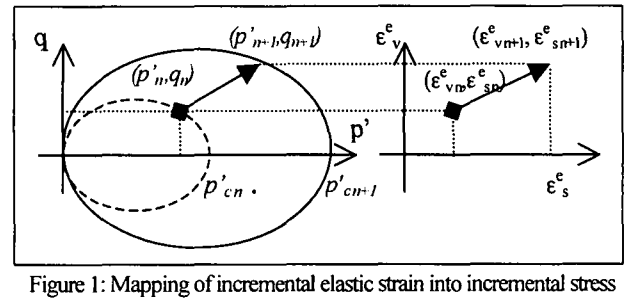

Figure 1: Mapping of incremental elastic strain into incremental stress

According to the stored energy in Eq.(4.14-4.15), the inelastic damage process affects on deviatoric stress when stress is in contact with yield surface. Refer to Eq.(4.16, 4.24), the quotient of incremental relation between q and p'_c are expressed by,

$$\frac{\delta q}{\delta p'_c} = \frac{3G(p'_c)\delta\varepsilon_s^e}{\frac{p'_o}{\bar{\kappa}} \exp(\frac{\varepsilon_{vc}^e}{\bar{\kappa}}) \delta\varepsilon_{vc}^e} = 3\mu' \frac{\delta\varepsilon_s^e}{\delta\varepsilon_{vc}^e} \quad (5.5)$$

It is assumed that a material experiences a holonomic strain path; i.e., proportional increments of strain over the time interval, thus, the explicitly integrated expression can be evaluated by considering an incremental elastic strain as shown in Fig.1 from

initial yield stress (step n) to a subsequent yield stress (step n+1).

$$\frac{q_{n+1}-q_n}{p'_{cn+1}-p'_{cn}} = 3\mu' \frac{\varepsilon^e_{sn+1}-\varepsilon^e_{sn}}{\varepsilon^e_{vcn+1}-\varepsilon^e_{vcn}} \tag{5.6}$$

Manipulate Eq.(5.6) and use Eq.(3.3), the nonlinear secant shear modulus including damage process due to a change in size of yield surface can be determined by,

$$\frac{q_{n+1}-q_n}{\varepsilon^e_{sn+1}-\varepsilon^e_{sn}} = 3\mu' \frac{p'_{cn+1}-p'_{cn}}{\varepsilon^e_{vcn+1}-\varepsilon^e_{vcn}} = 3G_s(p'_{cn+1}, p'_{cn}) \tag{5.7}$$

where $$G_s(p'_{cn+1}, p'_{cn}) = \mu' \frac{p'_{cn+1}-p'_{cn}}{\bar{\kappa}\ln(p'_{cn+1}/p'_{cn})} \tag{5.8}$$

Non-linear secant shear modulus is a result of externally integrating on the plastic hardening parameter. It is noted that the secant shear modulus is held constant inside the state boundary. In case of the initial yield surface, the secant shear modulus is the tangent shear modulus of pre-consolidated pressure.

$$\lim_{p'_c \to p'_o} G_s(p'_c, p'_o) = G(p'_o) = \mu' \frac{p'_o}{\bar{\kappa}} \tag{5.9}$$

By rewriting Eq.(5.7), Eq.(5.10) gives an evolution of q in Eq.(4.16) and stiffness matrix in Eq.(4.19) are thus taking damage effect into account.

$$q_{n+1} = q_n + 3G_s(p'_{cn+1}, p'_{cn})\left(\varepsilon^e_{sn+1} - \varepsilon^e_{sn}\right) \tag{5.10}$$

$$\mathbf{C} = \begin{bmatrix} \frac{p'_{n+1}}{\bar{\kappa}} & 0 \\ 0 & 3G_s(p'_{cn+1}, p'_{cn}) \end{bmatrix} \tag{5.11}$$

The relevant equations are summarized in Box 2.

Box 2: Elastic parameters and moduli

Recompressibility index: $\bar{\kappa} = \dfrac{\kappa}{1+e_o}$

Compressibility index: $\bar{\lambda} = \dfrac{\lambda}{1+e_o}$

Ratio of shear to bulk moduli: $\mu' = \dfrac{3(1-2\nu')}{2(1+\nu')}$

Tangent bulk modulus: $K(p') = \dfrac{p'}{\bar{\kappa}}$

Tangent shear modulus: $G(p'_c) = \mu' \dfrac{p'_c}{\bar{\kappa}}$

Secant shear modulus:

$$G_s(p'_{cn+1}, p'_{cn}) = \mu' \frac{p'_{cn+1}-p'_{cn}}{\bar{\kappa}\ln(p'_{cn+1}/p'_{cn})}$$

note: $G_s(p'_{cn}, p'_{cn}) = \mu' \dfrac{p'_{cn}}{\bar{\kappa}}$

6. Elastic constitutive equation

The incremental stress-strain relation can be described by,

$$\dot{\boldsymbol{\sigma}} = \mathbf{c}^e : \dot{\boldsymbol{\varepsilon}}^e \tag{6.1}$$

where $$\mathbf{c}^e = \frac{\partial \boldsymbol{\sigma}}{\partial \boldsymbol{\varepsilon}^e} = \mathbf{1} \otimes \frac{\partial p'}{\partial \boldsymbol{\varepsilon}^e} + \frac{\partial \mathbf{s}}{\partial \boldsymbol{\varepsilon}^e} \tag{6.2}$$

$$\boldsymbol{\sigma} = p'\mathbf{1} + \mathbf{s}, \quad \boldsymbol{\varepsilon}^e = \frac{1}{3}\varepsilon^e_v \mathbf{1} + \boldsymbol{\varepsilon}^e_d \tag{6.3a, b}$$

$$\frac{\partial p'}{\partial \boldsymbol{\varepsilon}^e} = \frac{\partial p'}{\partial \varepsilon^e_v}\frac{\partial \varepsilon^e_v}{\partial \boldsymbol{\varepsilon}^e} + \frac{\partial p'}{\partial \varepsilon^e_s}\frac{\partial \varepsilon^e_s}{\partial \boldsymbol{\varepsilon}^e_d} : \frac{\partial \boldsymbol{\varepsilon}^e_d}{\partial \boldsymbol{\varepsilon}^e} \tag{6.4}$$

$$\frac{\partial \mathbf{s}}{\partial \boldsymbol{\varepsilon}^e} = \frac{\partial \mathbf{s}}{\partial \varepsilon^e_v} \otimes \frac{\partial \varepsilon^e_v}{\partial \boldsymbol{\varepsilon}^e} + \frac{\partial \mathbf{s}}{\partial \varepsilon^e_s} \otimes \frac{\partial \varepsilon^e_s}{\partial \boldsymbol{\varepsilon}^e_d} : \frac{\partial \boldsymbol{\varepsilon}^e_d}{\partial \boldsymbol{\varepsilon}^e} + \frac{\partial \mathbf{s}}{\partial \hat{\mathbf{n}}} : \frac{\partial \hat{\mathbf{n}}}{\partial \boldsymbol{\varepsilon}^e_d} : \frac{\partial \boldsymbol{\varepsilon}^e_d}{\partial \boldsymbol{\varepsilon}^e} \tag{6.5}$$

$\mathbf{I} \equiv \frac{1}{2}\left[\delta_{ik}\delta_{jl} + \delta_{il}\delta_{jk}\right]\mathbf{e}_i \otimes \mathbf{e}_j \otimes \mathbf{e}_k \otimes \mathbf{e}_l$ is the forth-order identity tensor, $\mathbf{c}^e$ is forth-order tensor of elastic stiffness including damage effect. Elements of $\mathbf{C}$ are defined in Eq. (5.11). In this case, C_{12} and C_{21} are simply zero.

$$\mathbf{c}^e = C_{11}\mathbf{1} \otimes \mathbf{1} + \sqrt{\frac{2}{3}}C_{12}\mathbf{1} \otimes \hat{\mathbf{n}} + \sqrt{\frac{2}{3}}C_{21}\hat{\mathbf{n}} \otimes \mathbf{1} + \frac{2}{3}C_{22}\mathbf{A} \tag{6.6}$$

where $\mathbf{A} \equiv \mathbf{I} - \frac{1}{3}(\mathbf{1} \otimes \mathbf{1})$, $\hat{\mathbf{n}} = \dfrac{\mathbf{s}}{\|\mathbf{s}\|}$ (6.7a, b)

7. Integration schemes

Solutions of elasto-plastic responses usually rely on sub-stepping technique, however, a numerical result is inaccurate due to a drift on the yield function. By fully implicit integration (Backward-Euler), the state variables at current step are calculated and enforced to satisfy the yield function at the end of the step. Iterative methods based on this scheme are more robust, stable and give a better accuracy for the same increment of driving variables; e.g., strains, displacements, forces and time periods. It is necessary to integrate the constitutive equations by assuming material is subject to a constant rate of strain over the interested time interval. Elastic-plastic operator-splitting methodology is used in the fully implicit integrative scheme, leading to the return-mapping algorithms with unconditional stability and first-order accuracy[27].

Operator splitting theory has everything to do with a decomposition of incremental elastic and plastic parts. Fig. 2 illustrates an outline of the algorithm by referring to an elasto-perfectly-plastic one-dimensional model being pulled by force q on rough surface against friction resistance $\sigma_y=\mu p$. A slippage of box represents an irrecoverable deformation. A stretch of spring represents a recoverable deformation. The combined incremental deformation is split into two discrete steps. First is called elastic predictor step where plastic part is firmly locked and all deformation is dominated by trial elastic part. Second is called plastic corrector step where plastic part is released and elastic part is corrected. The box would stop at the stationary point where dissipation energy of a system reaches the maximum value and hence, the solution of a problem.

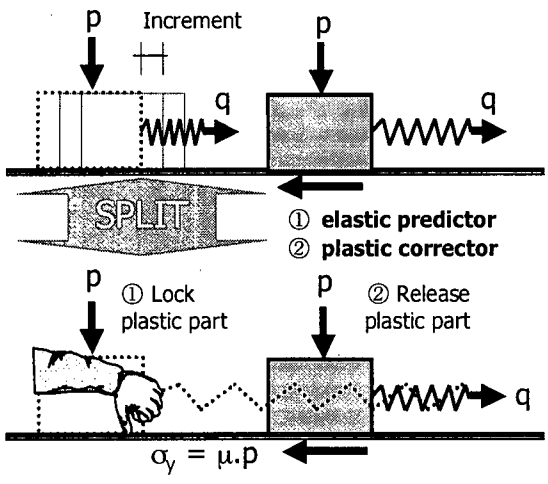

Figure 2: Schematization of operator-splitting theory

7.1 Time discretization

According to ordinary sub-incrementation technique for numerical integration, Forward-Euler difference is almost in practice giving the series of sub-increments. Though Backward-Euler difference is superior to that of explicit method by providing the iterative scheme with a quadratic rate of convergence, formulations driven by Forward-Euler are simpler than Backward-Euler, which is complex and depends crucially on the particular constitutive model chosen. Herein, the integration algorithm applicable to the Sekiguchi-Ohta model is presented. Refer to Eq.(2.10a),

$$\dot{\varepsilon}^e = \dot{\varepsilon} - \gamma \frac{\partial f}{\partial \sigma} \tag{7.1}$$

The integration to Eq.(7.1) within the time interval $[t_n t_{n+1}=t_n+\Delta t]$ can be approximated using Backward-Euler differential scheme where plastic strain increments and hardening variable are calculated at the end of the step.

$$\varepsilon_{n+1} = \varepsilon_n + \Delta\varepsilon, \quad \varepsilon^p_{n+1} = \varepsilon^p_n + \Delta\gamma_{n+1}\left\{\frac{\partial f}{\partial \sigma}\right\}_{n+1} \tag{7.2a, b}$$

where $\varepsilon_{n+1} = \varepsilon(t_{n+1})$, $\Delta\gamma_{n+1} = \gamma_{n+1}\Delta t$, $\Delta\varepsilon = \dot{\varepsilon}\Delta t$

Subtract Eq.(7.2a) by (7.2b) yields a current elastic strain tensor,

$$\varepsilon^e{}_{n+1} = \varepsilon^{tr} - \Delta\gamma_{n+1}\left\{\frac{\partial f}{\partial \sigma}\right\}_{n+1} \tag{7.3}$$

$$\varepsilon^{tr} = \varepsilon^e_n + \Delta\varepsilon \tag{7.4}$$

ε^{tr} is a trial strain given by geometric update of the imposed displacement increment over the time step. $\Delta\gamma$ is taken as zero in elastic predictor step. Stresses are updated correspondingly,

$$p'_{n+1} = p'_n \exp\left(\frac{\varepsilon^e_{vn+1} - \varepsilon^e_{vn}}{\bar{\kappa}}\right) \tag{7.5a}$$

$$s_{n+1} = s_n + 2G_s(p'_{cn+1}, p'_{cn})\left\{\varepsilon^e_{dn+1} - \varepsilon^e_{dn}\right\} \tag{7.5b}$$

Update state variables are summarized in Box 3.

7.2 Linearization

The goal of this section is to solve Eq.(7.3) for ε^e in strain space constrained by the discrete form of Kuhn-Tucker conditions given by

$$\Delta\gamma_{n+1} \geq 0\,;\, f_{n+1}(\sigma, p'_c) \leq 0\,;\, \Delta\gamma_{n+1}\cdot f_{n+1}(\sigma, p'_c) = 0 \tag{7.6}$$

The solution can be achieved iteratively by Newton-Raphson method assigned on a set of equations below with p'_c fixed.

$$\text{Unknown vector;} \qquad \mathbf{x} = \begin{Bmatrix} \varepsilon^e{}_{n+1} \\ \Delta\gamma_{n+1} \end{Bmatrix} \tag{7.7}$$

Eq.(7.3) and yield function define a residual vector of

$$\mathbf{r} = \begin{Bmatrix} \bar{\mathbf{r}} \\ f_{n+1} \end{Bmatrix} \text{ where } \bar{\mathbf{r}} = \varepsilon^e{}_{n+1} - \varepsilon^{tr} + \Delta\gamma_{n+1}\left\{\frac{\partial f}{\partial \sigma}\right\}_{n+1} \tag{7.8}$$

Consistent Jacobian of the residuals is defined by,

$$\left\{\frac{\partial \mathbf{r}}{\partial \mathbf{x}}\right\} = \begin{bmatrix} \mathbf{I} + \Delta\gamma\dfrac{\partial^2 f}{\partial\sigma\partial\sigma} : \mathbf{c}^e & \dfrac{\partial f}{\partial \sigma} \\ \dfrac{\partial f}{\partial \sigma} : \mathbf{c}^e & 0 \end{bmatrix}_{n+1} \tag{7.9}$$

$$\text{Iterative scheme;} \quad \mathbf{x}^{(k+1)} = \mathbf{x}^{(k)} - k_c\left\{\frac{\partial \mathbf{r}}{\partial \mathbf{x}}\right\}^{-1}\cdot\mathbf{r}^{(k)} \tag{7.10}$$

Super-script k indicates an iteration number. The iteration will stop when the norm of residual vector is less than the tolerance imposed. k_c denotes a controlled step of convergence. Iterative scheme in Eq.(7.10) can be reduced to the following procedures. The algorithmic moduli Ξ replace the Hessian matrix of the Lagrangian function by reassembling

$$\mathbf{I} + \Delta\gamma_{n+1}\left\{\frac{\partial^2 f}{\partial\sigma\partial\sigma}\right\}_{n+1} : \mathbf{c}^e_{n+1} = \Xi^{-1}_{n+1} : \mathbf{c}^e_{n+1} \tag{7.11}$$

$$\text{Therefore,} \quad \Xi_{n+1} = \left(\mathbf{c}^e_{n+1}{}^{-1} + \Delta\gamma_{n+1}\mathbf{H}_{n+1}\right)^{-1} \tag{7.12}$$

where $\mathbf{H}_{n+1} = \left\{\dfrac{\partial^2 f}{\partial\sigma\partial\sigma}\right\}_{n+1}$ and $\mathbf{h}_{n+1} = \left\{\dfrac{\partial f}{\partial\sigma}\right\}_{n+1}$

The different of unknown vector for each iteration can be expressed by Eq.(7.13). Substitute Eq.(7.13) into Eq.(7.10) and rearrange to form Eq.(7.14),

$$\mathbf{x}^{(k+1)} - \mathbf{x}^{(k)} = \begin{Bmatrix} \delta\varepsilon^e \\ \delta\Delta\gamma \end{Bmatrix} \tag{7.13}$$

$$\begin{bmatrix} \Xi^{-1} : \mathbf{c}^e & \mathbf{h} \\ \mathbf{h} : \mathbf{c}^e & 0 \end{bmatrix}_{n+1} \begin{Bmatrix} \delta\varepsilon^e \\ \delta\Delta\gamma \end{Bmatrix} = -k_c \begin{Bmatrix} \bar{\mathbf{r}} \\ f \end{Bmatrix}_{n+1} \tag{7.14}$$

Pre-multiply the first set of Eq.(7.14) by $\{\mathbf{h} : \Xi\}_{n+1}$, then

$$\left\{\mathbf{h}:\mathbf{c}^e:\delta\boldsymbol{\varepsilon}^e+\delta\Delta\gamma\mathbf{h}:\boldsymbol{\Xi}:\mathbf{h}\right\}_{n+1}=-k_c\left\{\mathbf{h}:\boldsymbol{\Xi}:\bar{\mathbf{r}}\right\}_{n+1} \quad (7.15)$$

$$\left(\mathbf{h}:\mathbf{c}^e:\delta\boldsymbol{\varepsilon}^e\right)_{n+1}=-k_c f_{n+1} \quad (7.16)$$

Solve for $\delta\Delta\gamma$ by substituting R.H.S of Eq.(7.16) to Eq.(7.15). $\delta\varepsilon^e$ can be solved by substitution of $\delta\Delta\gamma$ in Eq.(7.15) to the first set of Eq.(7.14). The difference of the increments of consistency parameter and elastic strain are as follow,

$$\delta\Delta\gamma=k_c\left(\frac{f-\mathbf{h}:\boldsymbol{\Xi}:\bar{\mathbf{r}}}{\mathbf{h}:\boldsymbol{\Xi}:\mathbf{h}}\right)_{n+1} \quad (7.17)$$

$$\delta\boldsymbol{\varepsilon}^e=\left\{-\mathbf{c}^{e^{-1}}:\boldsymbol{\Xi}\left(k_c\bar{\mathbf{r}}+\delta\Delta\gamma\mathbf{h}\right)\right\}_{n+1} \quad (7.18)$$

According to the previous research[14], a controlled-step of convergence is suggested by $k_c=3/4$ to refrain iteration from the ill convergent direction. Update the unknown variables by,

$$\Delta\gamma_{n+1}^{(k+1)}=\Delta\gamma_{n+1}^{(k)}+\delta\Delta\gamma \quad (7.19)$$

$$\boldsymbol{\varepsilon}^{e(k+1)}_{n+1}=\boldsymbol{\varepsilon}^{e(k+1)}_{n}+\delta\boldsymbol{\varepsilon}^e \quad (7.20)$$

$$\varepsilon_{vn+1}^{e(k+1)}=tr(\boldsymbol{\varepsilon}^{e(k+1)}_{n+1}),\quad \varepsilon_{dn+1}^{e(k+1)}=\mathbf{A}:\boldsymbol{\varepsilon}^{e(k+1)}_{n+1} \quad (7.21a,\ b)$$

$$\varepsilon_{vn+1}^{p(k+1)}=tr\left(\boldsymbol{\varepsilon}_{n+1}-\boldsymbol{\varepsilon}^{e(k+1)}_{n+1}\right) \quad (7.22)$$

$$p'^{(k+1)}_{cn+1}=p'_{cn}\exp\left(\frac{\varepsilon_{vn+1}^{p(k+1)}-\varepsilon_{vn}^{p}}{\bar{\lambda}-\bar{\kappa}}\right) \quad (7.23)$$

$$p'^{(k+1)}_{n+1}=p'_{n}\exp\left(\frac{\varepsilon_{vn+1}^{e(k+1)}-\varepsilon_{vn}^{e}}{\bar{\kappa}}\right) \quad (7.24)$$

$$\mathbf{s}^{(k+1)}_{n+1}=\mathbf{s}_n+2G_s(p'^{(k+1)}_{cn+1},p'_{cn})\left\{\boldsymbol{\varepsilon}_{dn+1}^{e(k+1)}-\boldsymbol{\varepsilon}_{dn}^{e}\right\} \quad (7.25)$$

The iterative loop of Eq.(7.10) corresponds to the Closest Point Projection (CPP) method. To bypass the need for computing the gradients in Eq.(7.9), Cutting-Plane (CP) method using an explicit procedure is developed involving quasi-Newton method[6]. CP algorithm applicable to the Sekiguchi-Ohta is available in the previous research[14]. It is obvious that CPP is superior to CP in accuracy and stability in particular for a large step increment[9]. Box 4 contains detailed procedures of single/multiple-step CPP method.

Box 3: Updated state variables

Stress update

$$p'_{n+1}=p'_n\exp\left(\frac{\varepsilon_{vn+1}^{e}-\varepsilon_{vn}^{e}}{\bar{\kappa}}\right)$$

$$\mathbf{s}_{n+1}=\mathbf{s}_n+2G_s(p'_{cn+1},p'_{cn})\left\{\boldsymbol{\varepsilon}_{dn+1}^{e}-\boldsymbol{\varepsilon}_{dn}^{e}\right\}$$

Stress-hardening parameter update

$$p'_{cn+1}=p'_n\exp\left(\frac{\varepsilon_{vn+1}^{p}-\varepsilon_{vn}^{p}}{\bar{\lambda}-\bar{\kappa}}\right)$$

8. Numerical examples

In order to evaluate the performance of the algorithm, the numerical examples based on two-invariant stress space problem of consolidated undrained test (CU test) and unconsolidated undrained test (UU test) were performed by a strain-controlled axial compression to a maximum axial strain of 10%. Soil parameters were adopted from soil reports of the northern line of Bangkok initial subway project[28]. The systematic parameter determination suggested by Iizuka and Ohta[29] (1987) was used to determine soil parameters for calculation as listed in Table 1. The tolerances, TOL_1 and $TO\ L_2$, were set to 10^{-5}. Verification was done by comparisons with a closed-form solutions derived from the constitutive equations as well as exact results of both sub-stepping (SS) and CPP methods generated by a series of very small increments of imposed strain.

Table 1: Soil parameters

Parameter	Description	Value
D	Coefficient of dilatancy	0.102
Λ	Irreversibility ratio	0.825
M	Critical state parameter	1.12
ν'	Effective Poisson's ratio	0.38
K_o	Coefficient of earth pressure (NC)	0.61
K_i	Coefficient of earth pressure (in-situ)	0.70
λ	Compression index	0.376
e_o	Void ratio at σ'_{vo}	1.735
σ'_{vo}	Eff. preconsolidation pressure (kN/m^2)	100
σ'_{vi}	Eff. overburden pressure (kN/m^2)	69

8.1 Accuracy assessment

In practice, the number of sub-increments is repeatedly applied to algorithms for improving the accuracy. To evaluate the calculation performance, a series of analyzes were performed for CU test by SS (using Forward-Euler difference) and CPP methods (using Backward-Euler difference) with a single step and incrementally multiple steps:- 5, 20, 50 and 1000 steps, in other words, with strain increments:- 2%, 0.5%, 0.2% and 0.01% respectively. The closed-form solutions relevant to the problem can be derived by directly integrating the constitutive equations over the imposed stress paths. These solutions are given for deviatoric stress and axial strain as functions of effective mean stress shown in Eq.(8.1,8.2). The comparisons with SS and CPP methods are arranged in Fig. 3.

$$q=\left(\eta_o-\frac{M}{\Lambda}\ln\left(\frac{p'}{p'_o}\right)\right)p' \quad (8.1),\ (8.2)$$

$$\varepsilon_a=\left(1-\left(\frac{p'}{p'_o}\right)^{\frac{1}{\Lambda}}\right)\left(\frac{\bar{\kappa}\Lambda}{3\mu'}\left(\frac{\bar{\kappa}}{D}-\eta_o\right)\right)+\frac{\bar{\kappa}\Lambda}{M}\ln\left(\frac{\left(\frac{p'}{p'_o}\right)^{\frac{-M^2}{3\mu'\Lambda}\left(\frac{p'}{p'_o}\right)^{\frac{1}{\Lambda}}}}{1+\frac{M}{\Lambda(M-\eta_o)}\ln\left(\frac{p'}{p'_o}\right)}\right)$$

Box 4: Closest Point Projection iterative scheme

1. Input: $\delta\boldsymbol{\varepsilon}, \boldsymbol{\sigma}_n, \boldsymbol{\varepsilon}_n, \boldsymbol{\varepsilon}^p_n, p'_{cn}$

2. Initialize: $k = 0$, $\Delta\gamma^{(k)}_{n+1} = 0$

$$\boldsymbol{\varepsilon}^e_n = \boldsymbol{\varepsilon}_n - \boldsymbol{\varepsilon}^p_n, \quad \boldsymbol{\varepsilon}_{n+1} = \boldsymbol{\varepsilon}_n + \delta\boldsymbol{\varepsilon}, \quad \delta\boldsymbol{\varepsilon}^{p(k)}_{n+1} = \mathbf{0}$$

$$\varepsilon_{vn+1} = tr(\boldsymbol{\varepsilon}_{n+1}), \quad \boldsymbol{\varepsilon}_{dn+1} = \mathbf{A} : \boldsymbol{\varepsilon}_{n+1}, \quad \hat{\mathbf{n}}_{n+1} = \frac{\boldsymbol{\varepsilon}_{dn+1}}{\|\boldsymbol{\varepsilon}_{dn+1}\|}$$

$$\varepsilon^e_{vn} = tr(\boldsymbol{\varepsilon}^e{}_n), \quad \boldsymbol{\varepsilon}^e_{dn} = \mathbf{A} : \boldsymbol{\varepsilon}^e{}_n, \varepsilon^p_{vn} = tr(\boldsymbol{\varepsilon}^e{}_n)$$

3. Elastic predictor:

$$\boldsymbol{\varepsilon}^{tr} = \boldsymbol{\varepsilon}^e_n + \delta\boldsymbol{\varepsilon}, \quad \boldsymbol{\varepsilon}^{e(k)}_{n+1} = \boldsymbol{\varepsilon}^{tr}, \quad \boldsymbol{\varepsilon}^{p(k)}_{n+1} = \boldsymbol{\varepsilon}^p_n + \delta\boldsymbol{\varepsilon}^{p(k)}_{n+1}$$

$$\varepsilon^{e(k)}_{vn+1} = tr(\boldsymbol{\varepsilon}^{e(k)}_{n+1}), \quad \boldsymbol{\varepsilon}^{e(k)}_{dn+1} = \mathbf{A} : \boldsymbol{\varepsilon}^{e(k)}_{n+1}$$

$$\varepsilon^{p(k)}_{vn+1} = tr(\boldsymbol{\varepsilon}^{p(k)}_{n+1}), \quad \boldsymbol{\varepsilon}^{p(k)}_{dn+1} = \mathbf{A} : \boldsymbol{\varepsilon}^{p(k)}_{n+1}$$

$$p'^{(k)}_{cn+1} = p'_{cn} \exp\left(\frac{\varepsilon^{p(k)}_{vn+1} - \varepsilon^p_{vn}}{\bar{\lambda} - \bar{\kappa}}\right)$$

$$p'^{tr} = p'^{(k)}_{cn+1} = p'_n \exp\left(\frac{\varepsilon^{e(k)}_{vn+1} - \varepsilon^e_{vn}}{\bar{\kappa}}\right)$$

$$\mathbf{s}^{tr} = \mathbf{s}^{(k)}_{n+1} = \mathbf{s}_n + 2G_s(p'^{(k)}_{cn+1}, p'_{cn})\left\{\boldsymbol{\varepsilon}^{e(k)}_{dn+1} - \boldsymbol{\varepsilon}^e_{dn}\right\}$$

$$\boldsymbol{\sigma}^{(k)}_{n+1} = p'^{(k)}_{n+1}\mathbf{1} + \mathbf{s}^{(k)}_{n+1}$$

4. Check yield function and residuals:

$$f_{n+1} = \mathrm{f}(\boldsymbol{\sigma}^{(k)}_{n+1}, p'^{(k)}_{cn+1})$$

$$\mathbf{h}_{n+1} = \left\{\frac{\partial f}{\partial \boldsymbol{\sigma}}\right\}_{n+1}, \quad \mathbf{H}_{n+1} = \left\{\frac{\partial^2 f}{\partial \boldsymbol{\sigma}\partial\boldsymbol{\sigma}}\right\}_{n+1}$$

$$\bar{\mathbf{r}} = \boldsymbol{\varepsilon}^{e(k)}_{n+1} - \boldsymbol{\varepsilon}^{tr} + \Delta\gamma^{(k)}_{n+1}\mathbf{h}_{n+1}$$

IF $f_{n+1} < TOL_1$ AND $\|\bar{\mathbf{r}}\| < TOL_2$

THEN Set $(\bullet)_{n+1} = (\bullet)^{(k)}_{n+1}$ and GOTO 9

5. Algorithmic moduli:

$$\mathbf{c}^e_{n+1} = K(p'^{(k)}_{n+1})\mathbf{1} \otimes \mathbf{1} + 2G_s(p'^{(k)}_{cn+1}, p'_{cn})\mathbf{A}$$

$$\boldsymbol{\Xi}_{n+1} = \left(\mathbf{c}^{e\,-1}_{n+1} + \Delta\gamma^{(k)}_{n+1}\mathbf{H}_{n+1}\right)^{-1}$$

6. Plastic corrector:

$$\delta\Delta\gamma^{(k)}_{n+1} = k_c\left(\frac{f - \mathbf{h} : \boldsymbol{\Xi} : \bar{\mathbf{r}}}{\mathbf{h} : \boldsymbol{\Xi} : \mathbf{h}}\right)^{(k)}_{n+1}$$

$$\delta\boldsymbol{\varepsilon}^{e(k)}_{n+1} = \left\{-\mathbf{c}^{e\,-1} : \boldsymbol{\Xi}\left(k_c\bar{\mathbf{r}} + \delta\Delta\gamma\mathbf{h}\right)\right\}^{(k)}_{n+1}$$

7. Update solutions:

$$\boldsymbol{\varepsilon}^{e(k+1)}_{n+1} = \boldsymbol{\varepsilon}^{e(k)}_{n+1} + \delta\boldsymbol{\varepsilon}^{e(k)}_{n+1}, \quad \Delta\gamma^{(k+1)}_{n+1} = \Delta\gamma^{(k)}_{n+1} + \delta\Delta\gamma^{(k)}_{n+1}$$

$$\delta\boldsymbol{\varepsilon}^{p(k+1)}_{n+1} = \boldsymbol{\varepsilon}^{tr} - \boldsymbol{\varepsilon}^{e(k+1)}_{n+1}, \quad \boldsymbol{\varepsilon}^{p(k+1)}_{n+1} = \boldsymbol{\varepsilon}^p_n + \delta\boldsymbol{\varepsilon}^{p(k+1)}_{n+1}$$

$$\varepsilon^{e(k+1)}_{vn+1} = tr(\boldsymbol{\varepsilon}^{e(k+1)}_{n+1}), \quad \boldsymbol{\varepsilon}^{e(k+1)}_{dn+1} = \mathbf{A} : \boldsymbol{\varepsilon}^{e(k+1)}_{n+1}$$

$$\varepsilon^{p(k+1)}_{vn+1} = tr(\boldsymbol{\varepsilon}^{p(k+1)}_{n+1}), \quad \boldsymbol{\varepsilon}^{p(k+1)}_{dn+1} = \mathbf{A} : \boldsymbol{\varepsilon}^{p(k+1)}_{n+1}$$

$$p'^{(k+1)}_{cn+1} = p'_{cn} \exp\left(\frac{\varepsilon^{p(k+1)}_{vn+1} - \varepsilon^p_{vn}}{\bar{\lambda} - \bar{\kappa}}\right)$$

$$p'^{(k+1)}_{n+1} = p'_n \exp\left(\frac{\varepsilon^{e(k+1)}_{vn+1} - \varepsilon^e_{vn}}{\bar{\kappa}}\right)$$

$$\mathbf{s}^{(k+1)}_{n+1} = \mathbf{s}_n + 2G_s(p'^{(k+1)}_{cn+1}, p'_{cn})\left\{\boldsymbol{\varepsilon}^{e(k+1)}_{dn+1} - \boldsymbol{\varepsilon}^e_{dn}\right\}$$

$$\boldsymbol{\sigma}^{(k+1)}_{n+1} = p'^{(k+1)}_{n+1}\mathbf{1} + \mathbf{s}^{(k+1)}_{n+1}$$

8. Set $k = k + 1$ and GOTO 4

9. Output: $\boldsymbol{\sigma}_{n+1}, \boldsymbol{\varepsilon}_{n+1}, \boldsymbol{\varepsilon}^p_{n+1}, p'_{cn+1}$ and EXIT

The errors of analyzes are obviously found due to the effect of increment sizes. Therefore, the emphasis is placed on selecting the size of sub-incrementation for high accuracy. According to Fig. 3, it is clearly seen that solutions by SS are drifted from the yield surface while those of CPP are always constrained on it. That is why the accuracy performance of CPP is substantially superior to SS for coarse increments or even a single step increment however it becomes extremely laborious for a finer step using very small sub-increments. The exact solution can be obtained by repeatedly applying the increasing numbers of sub-increments to the algorithms until there is no change in results. For 0.01% strain increment (1000 steps), numerical solutions by both CPP and SS meet the closed-form solution, thus resulting in exact solution.

8.2 Convergence study

Fig. 4 and Fig. 5 show the effective stress and stress-strain responses for UU test predicted by multiple-step SS and single-step CPP methods. The convergence performance of CPP method was tested by a single increment as large as failure axial strain of 10%. The stress update iterations started from the initial stress state inside yield surface and then moved outside by elastic predictor step. The consistency condition iteratively corrected the state variables to return back to yield surface taking damage effect on stored energy into account while internal hardening variables were updated simultaneously along the return paths. The number of iterations to satisfy the tolerance was 12. Fig. 6 shows that the consistency parameters computed at successive iterations using the consistent Jacobian can approach to the solution with a quadratic rate of convergence.

8.3 Evaluation of error

The undrained shear strength, S_u, is able to determine by UU tests. Expression of undrained shear strength for ideal samples is given below (Ohta et al[30],1989).

$$\left(\frac{S_u}{\sigma'_{vo}}\right)_{ideal} = \frac{1+2K_o}{6} M \exp\left(-\Lambda + \frac{\Lambda}{M}\eta_o\right)\left(OCR\frac{1+2K_o}{1+2K_i}\right)^{\Lambda-1} \quad (8.3)$$

Table 2 shows the results of S_u, determined by SS and CPP methods with the variation of sub-increments. Errors are evaluated by comparison with Eq.(8.3). Though SS needs as much as 1000 steps for 0.20% accuracy, a single-step CPP method needs only 12 numbers of iteration for -0.77% accuracy. Therefore, CPP method is proved to give a high accuracy and stability even a single large strain near failure is imposed.

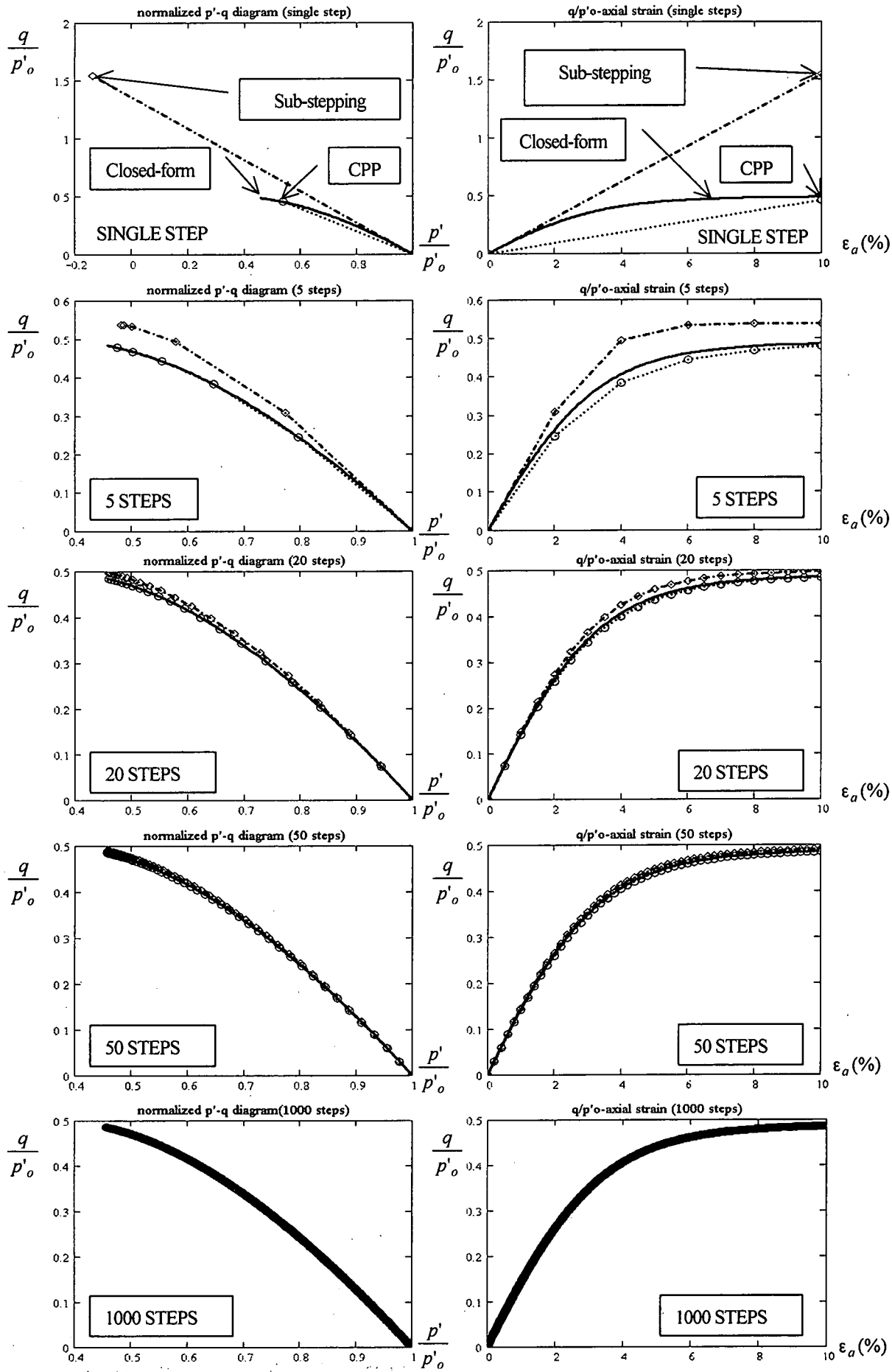

Figure 3: Numerical results for CU test generated by single/multiple step solutions by SS and CPP methods in compare with closed-form solution

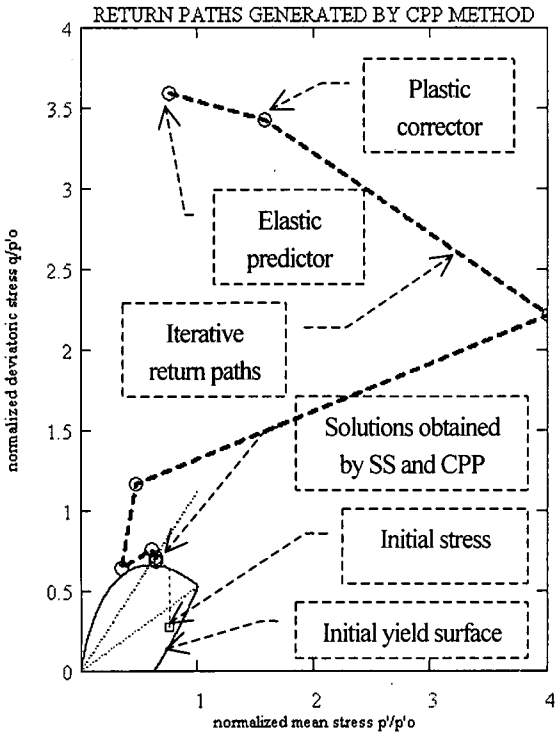

Figure 4: Numerical results by 1000-step SS and single-step CPP methods in p'-q space for UU test at 10% axial strain

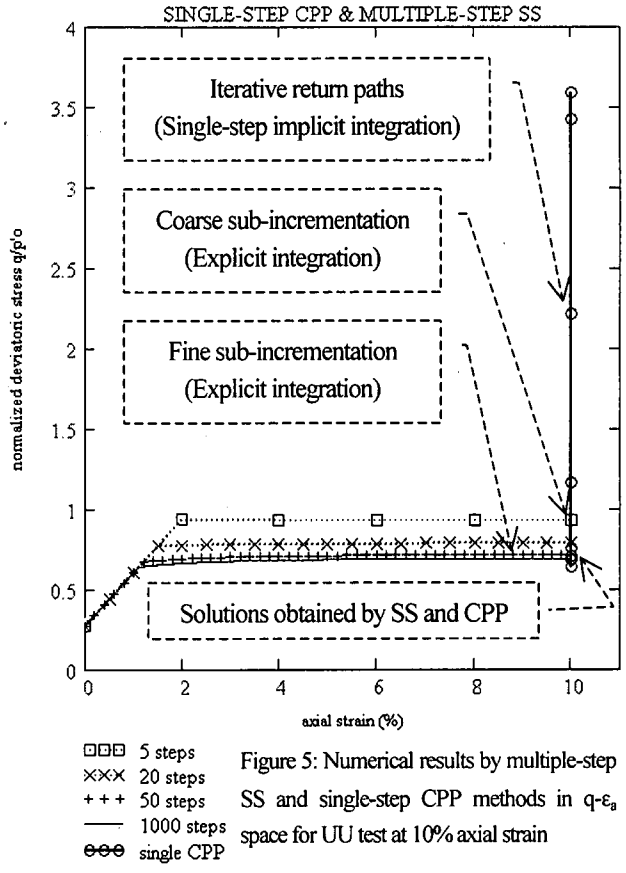

Figure 5: Numerical results by multiple-step SS and single-step CPP methods in q-ε_a space for UU test at 10% axial strain

Table 2: Undrained shear strength tests (10% axial strain)

Method	Normalized strength S_u/σ'_{vo}	Error (%)
Closed-form	0.2547	0.00
SS (single step)	1.3258	420.48
SS (5 steps)	0.3443	35.16
SS (20 steps)	0.2909	14.21
SS (50 steps)	0.2639	3.60
SS (1000 steps)	0.2552	0.20
CPP (single step)	0.2528	-0.77
CPP (5 steps)	0.2543	-0.17
CPP (20 steps)	0.2545	-0.04
CPP (50 steps)	0.2546	-0.03
CPP (1000 steps)	0.2547	-0.03

SS = Sub-Stepping, CPP = Closest Point Projection

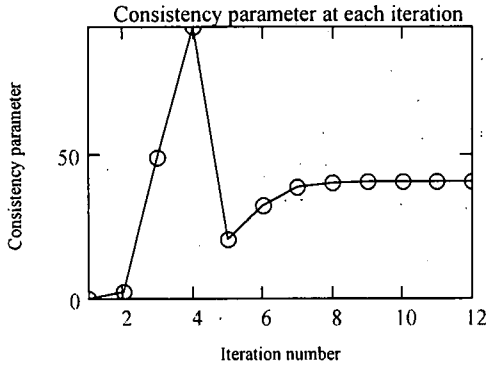

Figure 6: Convergence of consistency parameter approached by CPP algorithm for a single-step of 10% axial strain

9. Conclusion

The implicit integration algorithm cast in form of Closest Point Projection method in the context of strain-driven process for the inviscid Sekiguchi-Ohta model was developed. The two-invariant conservative stored energy function with damage process and choice of suitable hardening potential were proposed. A class of isotropic pressure-dependent bulk modulus and stress hardening parameter-dependent shear modulus were employed as an illustrative case of hyperelastic model required by return-mapping algorithms. The developed formulations were implemented and used in numerical analyses for CU and UU tests. The numerical results showed that CPP method could provide an effective, stable and robust integration scheme to the rate constitutive equations for any variation of imposed strain increments. The exact solutions of both CPP and SS methods can be obtained by subjecting the algorithms to very small strain increments. Verification has been done by comparisons with the closed-form solutions. The errors associates with CPP method were relatively low in compare with those of SS method even at a single large strain increment near failure. It was clear that CPP method is superior to SS method in particular when a small number of steps are applied or a large size of strain increments is used. The fundamental mathematical disciplines developed in the study will pave a way to a formulation of soil/water coupled FEM and the emerged evolution of finite deformation analysis in further research stages.

References

1) Sekiguchi, H. and Ohta, H., Induced anisotropy and time dependency in clays, *9th ICSMFE*, Tokyo, Constitutive equations of Soils, pp.229-238, 1977

2) Ohta, H. and Iizuka, A., *Ground Response to Construction Activities*, vol. 1&2, 1992

3) Nagtegaal, J.C. and De Jong, J.E., Some computational aspects of elastic-plastic large strain analysis, *Int. J. Num. Meth. Engrg. 17*, pp.15-41, 1981

4) Simo, J.C. and Hughes, T.J.R., *Computational inelasticity*, Springer, 1997

5) Suzuki, Y. and Aoyagi, R., A note on Simo's papers, private communication, 1999

6) Simo, J.C. and Ortiz, M., A unified approach to finite deformation elastoplastic analysis based on the use of hyperelasticity constitutive equations, *Comput. Methods Appl. Mech. Engrg. 49*, pp.221-245, 1985

7) Simo, J.C., Kennedy, J.G. and Govindjee, S., Non-smooth multisurface plasticity and viscoplasticity. Loading/unloading conditions and numerical algorithms, *Int. J. Numer. Methods Engrg. 26*, pp.2161-2185, 1988

8) Simo, J.C., Algorithms for static and dynamic multiplicative plasticity that preserve the classical return mapping schemes of the infinitesimal theory, *Comput. Methods Appl. Mech. Engrg. 99*, pp.62-112, 1992

9) Simo, J.C., Meschke, G., A new class of algorithms for classical plasticity extended to finite strains. Application to geomaterials, *Comput. Mech. 11*, pp.253-278, 1993

10)Borja, R.I. and Lee, S.R., Cam-Clay plasticity, Part I: Implicit integration of elasto-plastic constitutive relations, *Comput. Methods Appl. Mech. Engrg. 78*, pp.49-72, 1990

11)Borja, R.I., Cam-Clay plasticity, Part II: Implicit integration of constitutive equation based on a nonlinear elastic stress predictor, *Comput. Methods Appl. Mech. Engrg. 88*, pp.225-240, 1991

12)Borja, R.I. and Tamagnini, C., Cam-Clay plasticity, Part III: Extension of the infinitesimal model to include finite strains, *Comput. Methods Appl. Mech. Engrg. 155*, pp.73-95, 1998

13)Borja, R.I., Chao-Hua, L. and Francisco, J.M., Cam-Clay plasticity, Part IV: Implicit integration of anisotropic bounding surface model with nonlinear Hyperelasticity and ellipsoidal loading function, *Comput. Methods Appl. Mech. Engrg. 190*, pp.3293-3323, 2001

14)Pipatpongsa, T. and Ohta, H., Return-mapping algorithm for Sekiguchi-Ohta model, *2nd Inter. Summer Sym.*, JSCE, pp.229-232, 2000

15)Pipatpongsa, T., Ohta, H., Kobayashi, I. and Iizuka, A., Associated plastic flow at the intersection corner of plastic potential functions in soil mechanics, *Proc. of 36th Japanese Nat. Conf. on Geotech. Engrg*, pp.935-936, 2001

16)Pipatpongsa, T., Ohta, H., Kobayashi, I. and Iizuka, A., Dependence of K_o-value on effective internal friction angle in regard to the Sekiguchi-Ohta model, *Proc. of 36th Japanese Nat. Conf. on Geotech. Engrg*, pp.936-937, 2001

17)Pipatpongsa, T., Kobayashi, I., Ohta, H., and Iizuka, A., The vertex singularity in the Sekiguchi-Ohta model, *56th JSCE Annual Meeting*, in press, 2001

18)Pipatpongsa, T., Ohta, H., Kobayashi, I. and Iizuka, A., Integration algorithms for soil constitutive equations with a singular hardening vertex, *3rd Inter. Summer Sym.*, JSCE, in press, 2001

19)Hill, R., The mathematical theory of plasticity, *Oxford University Press, Oxford, U.K.*, 1950

20)Drucker, D.C., Some implications of work hardening and ideal plasticity, *Quart. Appl. Math. 7*, pp.411, 1950

21)Atkinson, J.H., *An Introduction to the Mechanics of Soils and Foundations*, McGRAW-HILL, London, 1993

22)Zytynski, M., Randolph, M.K., Nova, R., and Wroth, C.P., On modeling the unloading-reloading behaviour of soils, *Int. J. Numer. Anal. Methods Geomech. 2*, pp.87-93, 1978

23)Hueckel, T., Tutumluer, E., and Pellegrini, R., A note on non-linear elasticity of isotropic overconsolidated clays, *Int. J. Numer. Anal. Methods Geomech. 16(8)*, pp.603-618, 1992

24)Potts, D.M. and Ganendra, D., An evaluation of substepping and implicit stress point algorithms, *Comput. Methods Appl. Mech. Engrg. 119*, pp.341-354, 1994

25)Houlsby, G.T., The use of variable shear modulus in elastic-plastic models for clays, *Comp. And Geotech. 1*, pp.3-13, 1985

26)Borja, R.I., Claudio, T. and Angelo A., Coupling plasticity and energy-conserving elasticity models for clays, *Journal of Geotechnical and Geoenvironmental Engineering 123(10)*, pp.948-957, 1997

27)Ortiz, M. and Popov, E.P., Accuracy and stability of integration algorithms for elastoplastic constitutive relations, *Int. J. Numer. Methods Engrg. 21*, pp.1561-1576, 1985

28)ION · Joint Venture, MRTA ISP-North Contract, Intepretative Geotechnical Report, Vol 1, *Ove Arup & Partners International LTD.*, 1998

29)Iizuka, A. and Ohta, H., A determination procedure of input parameters in elasto-viscoplastic finite element analysis, *Soils and Foundations, Vol. 27(3)*, pp. 71-87, 1987

30)Ohta, H., Nishihara, A, Iizuka, A., Morita, Y., Fukagawa, R. and Arai, K., Unconfined compression strength of soft clays, *Proc. 12th Int. Conf. Soil Mech. & Foundation Engrg. Rio de Janeiro, Vol. 1*, pp.71-74, 1989

(Received: April 20, 2001)